UNIVERSIDADE DE SÃO PAULO

INSTITUTO DE FÍSICA
CAIXA POSTAL 20516
01000 - SÃO PAULO - SP
BRASIL

publicações

IFUSP/P-355

POINT DEFECT AGGREGATES IN BORON DOPED DISLOCATION-FREE CZOCHRALSKI SILICON CRYSTALS

by

Cecília A. Pimentel and C. Brito Filho

Instituto de Física, Universidade de São Paulo,
C. Postal 20516, 05508 São Paulo, Brasil

Agosto/1982

POINT DEFECT AGGREGATES IN BORON DOPED DISLOCATION-FREE CZOCHRALSKI SILICON CRYSTALS

Cecília A. Pimentel and C. Brito Filho
Instituto de Física da Universidade de São Paulo,
C. Postal 20.516, 05508 São Paulo, Brasil

ABSTRACT

Bragg line profile (BLP) and high-resolution diffuse X-ray scattering (DXS) measurements have been obtained in boron Czochralski Si single crystals. The crystals, dislocation free, doped with B concentration (C_B) from 10^{14} to 10^{19} cm^{-3}, have been analysed in a double crystal diffractometer using a highly collimated $CuK\alpha_1$ radiation. The BLP evidenced that the (111) plane is the most affected by doping process and in a more critical way for $C_B \gtrsim 10^{18}$ cm^{-3}. DXS results have shown the presence of clusters with typical size parameters of some tens to some thousands of angstrons with a prevaling interstitial-nature for the larger and vacancy-nature for the smaller, except for $C_B \sim 10^{19}$ cm^{-3} which presents only an interstitial-nature.

INTRODUCTION

Point defects are known to have marked effects on physical properties of silicon single crystals. Silicon crystals can be grown from the melt by means of the floating-zone (FZ) and Czochralski (CZ) techniques, free of line dislocations and macroscopic defects like twins and stacking faults [1]. During the growth, point defects can be inhomogeneously incorporated in the crystal and point defects agglomerates are often formed. The main defects and inhomogeneities occuring in Si crystals are: striations, corresponding to microscopically non-uniform spatial distribution of impurities (dopant, carbon, oxygen); microdefects or swirl defects, corresponding to agglomerates of atomic point defects, like silicon interstitials, vacancies; precipitates of impurities, e.g. oxygen precipitates in CZ silicon [1]. The performance of silicon electronic devices is significantly influenced by the presence of these microdefects and despite of extensive studies, many aspects regarding their nature and origin are still not understood. (For a review, see references [1-5]).

These silicon defects, that show a marked relation with the growth conditions [6], have been extensively studied in FZ-silicon. Only recently microdefects were detected in CZ-silicon [7,8]; three types of microdefects were found differing in size, density and spacial distribution: the larger, A-type, are perfect dislocation loops of interstitial nature; B-type are precipitate particles exhibiting a vacancy-type strain field; C-type, the smaller, are of character still not unravelled. Doping and crystal pulling rate (V_g) were found to affect strongly the formation of swirl defects in CZ silicon crystals [7,8].

Undoped or lightly doped (n- or p-type impurities) CZ crystals pulled at rates $V_g \leq 1$ mm/min contain the three types of microdefects distributed in striated patterns. At $V_g \gtrsim 2$ mm/min, A defect formation is completely suppressed. For concentrations exceeding 10^{17} cm^{-3}, the defect formation is drastically affected by the type of impurities: doping with acceptor type (B, Ga) suppresses completely the formation of B defects as well as of C defects; doping with donor type (Sb, P, As) eliminates the A defects. Similarly for FZ silicon, the carbon content of the crystals influences the concentration of B and C defects [8].

An accurate study of crystalline parameter variation of CZ silicon, boron doped by diffusion during the growth [9,10], has shown that the lattice interplanar spacings are differently contracted by the presence of boron. This preferential alteration occurs in a more pronunciate way for concentrations up to 10^{18} cm^{-3}; it was also observed a growth orientation dependence of the diffusion of boron.

These defects in Si single crystals have been characterized by means of several techniques: metal decoration combined with X-ray topography, etching, electron microscopy (TEM, HVEM, SEM-EBIC) and electrical measurements. The X-ray transmission topography is extensively employed but it does not allow a detailed characterization of the defect aggregates. On the other hand, the lattice strains due to point defects and clusters are sometimes very weak to produce visible images in X-ray topographs. The same occurs for B-swirl defects that have a weak strain field at room temperature, the attempts to identify them by TEM having failed [8].

In recent years, a very sensitive X-ray technique

has been employed in the study of point defects and their aggregates: the diffuse X-ray scattering technique [11]. The point defects and aggregates produce a diffuse X-ray scattering (DXS) near the Bragg reflection and the study of this DXS can give information about characteristics of those defects. DXS has been developed into a very powerful method for investigation of the structure and size of point defects and their agglomerates, being applicable for defect sizes ranging from single point defects up to dislocation loops which are large enough to be observed also in the electron microscope [12]. In order to study the DXS very near a Bragg reflection, accurate experimental conditions are required, such as highly collimated and monocromated X-ray beam [13-15] as well as precise mechanics apparatus to permit the rocking of the sample at very short steps. The high resolution technique for measurements of DXS has been particularly used by Lal and co-workers [14-21]. This method has been employed in detailed studies of point defect aggregates in nearly perfect silicon single crystal [16-18;20]; their interstitial or vacancy nature as well as the average cluster size were determined. As-grown silicon has showed DXS predominatingly due to aggregates of vacancies while the silicon, heated under oxygen, presents defect aggregates of interstitial type [18].

In the present paper the DXS technique is used in a high resolution condiction to study aggregates in Czochralski silicon single crystals, dislocation free, boron doped by diffusion during the growth. The doping levels, between 10^{14} and 10^{19} cm^{-3} are the generally used for CZ silicon device applications. It is also employed the profile analysis of Bragg reflection that can likewise gives information about the defects

in single crystals, despite of their yet qualitative aspect for some crystal defects [20-23].

OUTLINE OF THE METHOD

The basic theory of diffuse scattering from point defects and their aggregates has been discussed by several authors (for a review, see reference [11]). In this paper only the aspects used in the interpretation of the experimental results are discussed.

For statistically distributed point defects with small concentration c, the DXS depends directly on the number N of defects, the defect itself and the displaced cloud of lattice atoms in the vicinity of the defect. The DXS is measured as a function of the scattering vector $\underline{k}$ ($|\underline{k}| = (4\pi/\lambda)\mathrm{sen}\theta$); a $\underline{q}$ vector is defined as the difference between the scattering vector $\underline{k}$ and the nearest reciprocal lattice vector $\underline{h}$: $\underline{q} = \underline{k}-\underline{h}$. Depending on the deviation $\underline{q}$ from the Bragg reflection, two DXS regions are in general distinguished. For small $\underline{q}$, which means near to the Bragg reflections ($\underline{q} \ll \underline{h}$, $\underline{h} \simeq \underline{k}$), the DXS (or Huang scattering) intensity $I_H(\underline{q})$ varies as $1/q^2$, being determined by the behaviour of the long range displacement field of the defect. For large $\underline{q}$, the DXS intensity away from the Bragg reflections depends sensitively on the displacements in the immediate vicinity of the defect. In addition to the Huang scattering, there is a contribution to the intensity which varies like $1/q$, yielding an asymmetry of the DXS near the Bragg reflection. Therefore, the DXS intensity $I(\underline{q})$ is given by a symmetric $I_S(\underline{q})$ and a asymmetric $I_A(\underline{q})$ component; at small

$\underline{q}$ values, $I_S(\underline{q}) \simeq I_H(\underline{q})$. The sign of the antisymmetric term depends very sensitively on the strenghth of the displacement field: for dilation centers (e.g. vacancies) the DXS is more intense for angles smaller than the Bragg angle (θ_B) whereas for centers of compression it is more intense for angles larger than the Bragg angle.

When the N point defects are clustered together, there is a lower concentration of the new $N_{c\ell}$ defects given by $c_{c\ell} = c/n_{c\ell}$, where $n_{c\ell}$ is the number of point defects in the cluster; the $N_{c\ell}$ defects have a much stronger displacement field. The theory assumes a linear superposition of the displacements of the $n_{c\ell}$ point defects in a cluster, and also considers the scattering centers (clusters) statistically distributed and a constant density within a sphere of radius $R_{c\ell}$. For small $\underline{q}$ values, $|\underline{q}| \ll q_{cr} \simeq 1/R_{cr}$, R_{cr} being a critical cluster radius, the DXS intensity follows also the $1/q^2$ behaviour; this Huang scattering is very sensitive to defect clustering, increasing by a factor $n_{c\ell}$. For large $\underline{q}$ ($|\underline{q}| > q_{cr}$) values the DXS is determined by strongly distorted regions of the lattice, which means it is determined by the displacement field in the core of the cluster. An asymptotic displacement field is used since the $1/r^2$ behaviour of the long range displacement field is no longer followed and a generalized form of the Stokes-Wilson approximation can be applied. This DXS (or Stokes-Wilson scattering) intensity $I_{SW}(\underline{q})$ decreases very fast $\sim 1/q^4$ and is proportional to $c_{c\ell} \cdot n_{c\ell} = c$. A critical radius, $R_{cr} = 1/q_{cr}$, can be estimated, from the crossing point (q_{cr}) of the Huang and Stokes-Wilson scattering; at low reflection orders $R_{cr} \simeq R_{cluster}$ and this relations is often used for an estimate of the cluster radius.

Analogously to point defects, the asymmetric contribution to the DXS allows the determination of the type of cluster: vacancy, if higher intensity at $\theta < \theta_B$ and interstitial, if higher intensity at $\theta > \theta_B$.

Besides the evaluation of the cluster radius from the inverse of q_{cr} values, corresponding to the transition from Huang to Stokes-Wilson scattering, other propositions have been made. The rocking curves obtained in a double-crystal spectrometer with a wide-open counter is an integrated intensity, measured as a function of the deviation $\Delta\theta = \theta - \theta_B$ [11,24]; hence the DXS intensity must be integrate over all $\underline{q}$ values on the Ewald sphere surface. The result of this integration [11,24] takes into account the component of the $\underline{q}$ vector at the scattering beam direction, for a given deviation angle $\Delta\theta$: $|\underline{q}_o| = |\underline{h}|\ \Delta\theta\ \cos\theta = |\underline{q}|\ \cos\theta$. The symmetrical part of DXS intensity is given by:

$$I_S(q_o) \sim A\ \ell n\ (e^{1/2}/R_o q_o) \qquad \text{for} \qquad |\underline{q}| \leq 1/R_o$$

$$I_S(q_o) \sim C\left[1/R_o^2 q_o^2\right] \qquad \text{for} \qquad |\underline{q}| > 1/R_o \qquad \text{(Eq.1)}$$

where A includes the size and number of clusters and the wavelenght of the used radiation; and C includes the size of clusters and the employed $(hk\ell)$ reflection. To obtain the symmetrical part of the DXS intensity it is proposed [24,13] to consider the average of the intensity change measured at equal q_o or $\Delta\theta$ on either side of the center of Bragg peak ($\underline{k} = \underline{h} \pm q_o$). For $q < 1/R_o$, a plot of $I_S(q_o)$ vs. $\ell n\ q_o$ should be linear and yields an intercept ($I_S(q_o) = 0$) with the horizontal axis

of q which is $\approx 1/R_o$, i.e. the reciprocal of the cluster radius ($q_o = e^{1/2}/R_o$ (Eq.2)) [11]. For $q < 1/R_o$, a plot of $\ell n\ I_S(q_o)$ vs. $\ell n\ q_o$ should be linear with slope $m = -2$.

Another procedure is proposed by Lal and co-workers [17-19]. They have chosen an $I_S(q)$ vs. $1/q^2$ plot because a straight line is expected if the observed DXS corresponds to Huang scattering. For dislocation-free silicon single crystal they have observed that the plots are not single straight lines but consist of at least two straight lines with different slopes; the points where the lines change the slopes (or knee points, as called by Lal and co-workers) are important parameters since they can give information about the size of the clusters. These authors [18] also analysed the DXS intensity in a log $I_S(\underline{q})$ vs. log$(\underline{q})$ plot, which reveals regions of different values of n in the equation $I_S(q) = |\underline{q}|^{-n}$.

EXPERIMENTAL

The Czochralski silicon crystals used in the present investigation were grown in the Microelectronic Laboratory, Politechnic School, São Paulo University, and the wafers of normal semiconductor grade specifications belong to batches usually utilized in microcircuit devices. The crystals were grown in a purified argon atmosphere of low pressure (~13 Torr) at a pulling rate of about 1 mm/min. The silicon wafers have 4 cm in diameter, nominally 200 μm thick and the surface plane perpendicular to the growth direction (<001> and <111>). The usual chemical-mechanical polishing was made in order to remove the surface damage introduced by the cut process.

Several characteristics of the samples were obtained before the high resolution DXS study. Resistivity measurements (four point probe technique) were employed to assure the resistivity homogeneity (0.4 to 2.3%) and to obtain the concentration of electrically-active dopants. The thickness was determined by means of a capacitive process and showed an homogeneity of about 0.5%. A light interferometer was used to determine the radius of curvature: 25 m [9]; in some samples it was also evaluated from the diffraction curves obtained from a topographic camera, Lang-type: 400 m [25]. For B concentration higher than 10^{18} cm^{-3}, the doped silicon is completely absorvent to infrared radiation; therefore, it is impracticable the determination of residual carbon and oxygen contents in those crystals by the infrared absorption spectroscopic analysis. For the determination of carbon and oxygen content in a single crystal silicon P doped (6.5×10^{14} cm^{-3}), grown at the same usual conditions [26], the differential infrared technique was employed taking as standard a FZ-silicon (from General Diode Corp.), low carbon and oxygen concentrations, 200Ω.cm of resistivity; the obtained values of concentrations are 3×10^{17} cm^{-3} for oxygen and 10^{16} cm^{-3} for carbon. A profile analysis of Bragg reflection was carried out in a X-ray double diffractometer from different regions of the wafers in order to certify the crystalline homogeneity [20]. X-ray transmission topography in a Lang camera [25] has shown total absence of line dislocations as well as defects introduced by cut processes. The silicon specimens studied in this paper were also investigated by means of pseudo-Kossel technique [9,10] that likewise did not show the presence of dislocations. In Table 1 are shown the doped silicon samples, dislocation free, their direction of growth,

resistivity and boron concentration.

For the high resolution DXS measurements as well as to obtain the line profile of Bragg reflection (BLP) a double crystal diffractometer was mounted in such a way to profit some mechanics movements of a commercial Rigaku Denki diffractometer [20]. A schematic line diagram of the experimental arrangement is shown in Fig. 1a. It is employed a Cu radiation of a lineal section X-ray beam from a fine focus tube; the stability of the X-ray generator is 0.03%. To obtain the $K\alpha$ radiation it is used a single crystal monochromator, set in a special goniometer head. Platinum pinholes (ϕ = 200μm) allow the elimination of the $K\alpha_2$ radiation. The sample is mounted on a standard goniometer head of a Rigaku Denki full circle single crystal attachment, set in the comercial diffractometer. A scintillation counter is used as detector and a ω- or θ-scanning of the sample permits to obtain the BLP in a plotter or by counting the intensity step to step; a single-channel analyser is adjusted to utilize 90% of the energy spectrum. The mechanic stability of the arrangement was improved by adapting the diffractometer on an iron ground plate; this plate was projected in order also to allow the rotation of the diffractometer around the vertical axis of the monochromator. This disposability is particularly important in the initial stages of the alignment; on the other hand, it easily allows the utilization of others monochromator crystals. The alignment of the arrangement can be made in a very systematic and reproductive way, employing in the first stages a laser source in place of the detector. Figure 1b shows the BLP of the (111) reflection of Ge single crystal, obtained in the double crystal diffractometer, having a Ge (111) as monochromator; the half width of this BLP is 11 seconds of arc.

To possibilitate the record of such sharp line profiles it is necessary to adapt a gear reducer the θ-scanning motor axis of the diffractometer. A semi-automatic procedure possibilitates to get $\Delta\theta$ intervals of 2.5×10^{-4} degrees or less.

Particular care should be taken to centralize the sample. This is of fundamental importance for the BLP analysis [22] and for comparative analysis of high resolution DXS in different samples. The exact setting of the sample surface in the center of the full circle attachment is assured, by means of X-ray diffraction, after an accurate optical alignment to prevent geometric deformation in the BLP. Taking as references the (hkℓ) reflection of the surface plane, the crystal is adjusted until the [hkℓ] scattering vector is exactly perpendicular to the ω- or θ-rotation axis. This is verified from successive rotation of the sample around the [hkℓ] direction followed by the observation of the maximum or peak intensity. This intensity must be constant within the mechanic precision of the goniometer head movements. This procedure also allows to check the symmetry of the cut of the wafers, since asymmetries can alter the half width of the BLP. Within the precision of our measurements, was not detected alterations in the BLP of surface plane reflections of the studied crystals.

For the five samples it was obtained the BLP of nine reflections. For a qualitative control, they were recorded in a plotter at a condition of low time constant (0.5 s) and scanning speed ($1/16^{o}$/min). In the procedure of step by step counting it was employed constant time; different $\Delta\omega$ intervals were used in a profile. To avoid truncation errors in the BLP, the intensity measurements were made until the background counting is reached. The background is measured in both sides of each line

profile; for the background correction it is subtracted from each intensity value the correspondent background intensity, obtained for each reflection adjusting a straight line by least mean square. Care was taken to study the same set of (hkℓ) reflections in all the samples (and not the equivalent one {hkℓ} reflections). Besides the stability of the experimental arrangement, systematic verifications of the electronic conditions and the initial performance of the double crystal diffractometer were done, employing a standard reflection.

RESULTS AND DISCUSSION

In this paper the intensities always refer to relative intensity in arbitrary unities but its unity is the same for all BLP and DSX intensities, since in this experiment the intensity of the exploring X-ray beam is kept constant. DXS intensity is expected to contribute preferentialy to enlarge the base of BLP; therefore, it is considered more pertinent to take the width at half height to evaluate the profile width since the integral width would take into account also the DXS. Figure 2 shows the $\beta_{1/2}$ half-width values for several (hkℓ) relp's of free-dislocation doped silicon crystals with increasing boron concentration. An undoped silicon single crystal, ~ 400Ω.cm resistivity, from Hooboken, is taken as reference and the $\beta_{1/2}$ values from its reflections are also signalized in Fig. 2.

The diffractions curves are narrow, the $\beta_{1/2}$ for the various Si crystals varied in the range of 11" (Si 10^{14}, (111)) to 135" (Si 10^{19}, (440)). As a general tendency, it is observed an increasing of $\beta_{1/2}$ values as the C_B boron

concentration increases but two distinct behaviours of this parameter are evident, depending on C_B. Until $C_B \approx 10^{16}$ cm^{-3} the BLP are very sharp; the (hkℓ) BLP from Si 10^{14} and Si 10^{15} present nearly the same geometric parameters than the standard silicon reflections; the $\beta_{1/2}$ values show no significative alteration, being the (111) reflection the most affected, with an increasing of about 18% (11" to 13") in its $\beta_{1/2}$ value. Marked changing occurs for higher C_B values ($\sim 10^{18}$ cm^{-3}); taking as reference the standard silicon, the $\beta_{1/2}$ of (111) reflection from Si 10^{18} has increased by a factor 9.5. It is worthwhile to note that, at lower C_B values, an increasing in C_B of a factor 23 alters in 10% the $\beta_{1/2}$ value while at higher C_B values, an increasing of C_B of only a factor 3 also alters in 10% the same parameter $\beta_{1/2}$. Taking into account the broadening due to dispersion it is observed a preferential alteration in (hkℓ) BLP as the B concentration increases. The most affected reflections with the doping process are respectively, (111) - the most significantly changed - (220), (311) and (400).

These BLP results are in accordance with the results of precision interplanar spacing from the same silicon samples, employing pseudo-Kossel technique [9,10]: the B diffusion process was found to affect differently the crystallographic planes producing a contraction particularly in {333} planes and also, in a more pronunciate, way for concentrations over 10^{18} cm^{-3}.

It is considered of interest to analyse the DXS in this <111> crystallographic direction and the (111) and (333) reflections were chosen to be studied; the (111) reflection is the less affected by instrumental dispersion and the (333) is a high order reflection, very sensitive to crystal perfection.

A computer program was made to analyse the DXS and a collection of curves is obtained from a plotter. A typical sequence is illustrated in Fig. 3 for the (333) reflection from sample Si 10^4.

Fig. 3a shows the log I vs. log $|\underline{q}|$ plot where it is identified the q values corresponding to $\theta > \theta_B$ and $\theta < \theta_B$. These plots for (111) and (333) reflections from all the samples have presented regions of lineal behaviour with different slopes - m. Table 2 shows the m slope values corresponding to regions of $q < q_{cr}$ and $q > q_{cr}$ (hereafter called respectively H and S-W regions); for some plots, the lineal behaviours can only be admited at $q \lesssim q_{cr}$ and $q \gtrsim q_{cr}$. For samples with low C_B the (111) reflections have presented lineal behaviour with a $\sim q^{-2}$ decrease of the DXS in both H and S-W regions following, therefore, the Huang scattering law; from samples heavily doped it is observed in both regions a much slower decrease of DXS intensity with q ($q^{-1.2} - q^{-1.8}$), which may indicate that close to the defect the displacements are much large than in an r^{-2} extrapolations of long-range displacement field [27]. From all the samples, (333) reflections have presented a marked change in the behaviour of the DXS intensity with the increasing of q. From samples with low C_B the DXS intensity follows in H region the Huang scattering law (q^{-2} dependence) and in S-W region the Stokes-Wilson law (q^{-4} dependence); the average radius of clusters (R_{cr}) obtained from the crossing point of changing of behaviour q^{-2} to q^{-4} (Table 2) are of some hundred of angstrons. For samples with high C_B it is difficult to precise the slope in H region and only a tendency to a q^{-2} dependence is observed; in S-W region a more fast decrease of the intensity occurs, but less than q^{-3} (q^{-m}, $2.4 < m < 2.9$), which is a first indication of the q^{-4} dependence

observed for even stronger defects [26]; it is also noted a distint behaviour of the DXS intensity for q values corresponding to $\theta > \theta_B$ and $\theta < \theta_B$. Variation of the slopes in these plots with the orders of reflections has been pointed out [17,27]. The observed deviation from the q^{-2} law indicates that the nearest neighbors of the clusters are strongly distorted [11]; this distortion is quite different for the heavily doped samples and it is not possible from the crossing point to well define an average radius of clusters.

Fig. 3b expresses the I vs. $\ell n|\underline{q}_o|$. The behaviour of these curves is in accordance with theoretical prediction (Eq. (1)), being lineal near the peak, until a particular q_{cr} value. The alteration of the lineal behaviour is interpreted as due to a differential DXS, produced by strain fields internal and external to the cluster [11]. The symmetrical part of the DXS intensity (from Eq. (2)) is used to obtain the q_o value correspondent to the intersect of the straight line and the abcisse axis. From the q_o relation, the average size of the aggregates was evaluated. Table 2 shows the mean values of the clusters size R_o for the free-dislocation doped CZ-silicon single crystal with different B concentration. The R_o values obtained from (111) reflections are bigger than those from (333) reflections, which are more affected by the dispersion. There is a general tendency to a decreasing of the R_o value with the increasing of C_B. For very sharp BLP (like (111) reflections from Si 10^{14}, Si 10^{15} and Si 10^{16}), it is observed the close dependence of the slope of the straight line with the elimination of a few points very near to the Bragg peak. This fact yields a large imprecision in the determination of q_o. (This explains the two different values presented in Table 2

for a sample Si 10^{14}).

A comparison between the R_{cr} and R_o values obtained from (333) reflections shows $R_o = 3R_{cr}$ and, therefore, an occurance to a q^{-2} dependence at $q \gtrsim q_o$. The present results for (333) reflections are quite different from the obtained by Patel [13], under analogous experimental conditions, for Si crystals having about the same oxygen concentration but after heat treatment, which induces the oxygen to cluster. This author has observed a q^{-2} dependence of the DXS at $q > 1/R_o$ and oxygen cluster of size $R_o \approx 2{,}200$ Å. Therefore, the observed q dependences of DXS in the present paper are related to the presence of B and for all range of B concentration our results show clusters of size $R_o < 2{,}200$ Å.

Fig. 4c shows a typical plot of DXS intensity as function of $|\underline{q}|^{-2}$ (I vs. $1/q^2$). It represents a more efficient and sensible anamorphosis than the plot showed in Fig. 3a. These plots show that for a given value of $|\underline{q}|$, the correspondent intensity value $I(\underline{q})$ is different depending on observed directions. This behaviour strongly suggest that the results are predominantly due to defects aggregates [18]. The straight lines have different slopes, like observed by Lal and co-workers [17-19]. To obtain the correspondent q values from the knee points, care is taken to vary sucessively the vertical and horizontal scale of the plot to better define those points. Table 2 gives this parameter size for all the studied samples; it is wothwhile to point out that for a sample the set of radius values means the most prominent average values (R) for the size of clusters. It is observed, as a general tendency, an increasing in the number of R as the C_B increases; it is also noted the decreasing in the smaller values with the increasing og C_B,

which is in agreement to the results obtained for R_o .

The size parameter for the aggregates varies in a large range of values, from tens to thousands angstrons. In a similar DXS study of undoped silicon, Lal et al. [17] have obtained as typical size parameter for the aggregates, 3,000 to 10,000 Å. The presence of B has, therefore, marked influence in the range of cluster size values, particularly in the smaller ones.

To analyse the nature of the aggregates, it is considered the asymmetries in the DXS intensities in terms of the θ-angles, since in reciprocal space when $\theta > \theta_B$ (or $\theta < \theta_B$) $\underline{q}$ is parallel (or antiparallel) to $\underline{h}$. The plotting of intensity in a logarithmic scale (log I vs. $\Delta\theta$), as shown in Fig. 3d, gives a qualitative evidence of the presence of DXS in BLP. Fig. 4 allows to comparate the DXS of (111) and (333) reflections from the samples. These curves put also in evidence the anisotropies in the distribution of DXS intensity in both side of the BLP, taking as reference the Bragg angle θ_B. The evaluation of asymmetries were done from the BLP's and from the log I vs. $\log|\underline{q}|$ plots, taking into account the existence of the two H and S-W regions. These plots allow a better observation of changes in asymmetry with the increasing of q values, as can be seen in Fig. 3a. For the studied reflections it is determined the sign of that asymmetrical behavior that is related to vacancy or interstitial cluster type. Table 2 gives the predominante nature of the clusters in the doped CZ-silicon for several B concentrations, from the (111) and (333) reflections. From the less doped samples it is not evident in (111) reflections the presence of asymmetries in both H and S-W regions; therefore, no prevailing nature of clusters is observed. In the

(333) reflections the DXS intensity in H region is higher for $\theta > \theta_B$ than the $\theta < \theta_B$, the opposite occuring in S-W region; this behaviour is also observed in (111) and (333) reflections from sample Si 10^{18}; these asymmetries correspond to a prevailing interstitial-type cluster from H region and a vacancy one from S-W region. The DXS intensity from Si 10^{19} shows a distint behaviour: a predominant interstitial-type from (333) reflection in both H and S-W regions and from (111) only in S-W region since in H region a predominant vacancy-type is observed. (The experimental data of Si 10^{19} sample were analysed with a particular care in order to confirm the above results). It seems interesting to note that the inversion of asymmetry (that occurs for all reflections except (333)-Si 10^{19}) takes place at q values near to q_{cr} . Similar inversion of asymmetry was presented by Lal et al. [17], e.g. in Fig. 8a. If it is considered the (333) reflections, the prevailing nature of the clusters can be so summarized: until $C_B \sim 10^{18}$ cm^{-3} , interstitial-type in H region and vacancy-type in S-W regions; for $C_B \sim 10^{19}$ cm^{-3} , interstitial-type in both region. Considering the results from the I vs. $1/|\underline{q}|^2$ plots and the R_o and R_{cr} values it is possible to relate the interstitial- and vacancy-nature respectively to the larger and smaller clusters.

Fig. 4 puts also in evidence the relative increasing in the DXS intensity for different increasing of C_B , the largest alteration occuring from $C_B \sim 10^{16}$ to 10^{18} cm^{-3} ; the marked alteration in BLP width also occurs in this C_B range. As it was discussed in the outline of the method, the Huang scattering increases with the growth of clusters and the Stokes-Wilson scattering with the point defect concentration (c). A non linear increase of I_H with concentration is observed and the results

seems to indicate that for $C_B \sim 10^{18}$ cm^{-3}, besides an increasing of c, a sensitive process of clustering occurs.

SUMMARY

The BLP results have shown that until $C_B \sim 10^{16}$ cm^3, the crystalline quality of Czochralski silicon single crystals (V_g = 1 mm/min) is practically not affected by the B doping process. After that value the crystal begins, in a more pronunciate manner, to lose its crystalline perfection. The BLP analysis has shown the (111) plane as the most affected by doping process. The broadening of BLP due to internal stress is related to an increasing of the number of boron atoms in the silicon lattice, and in a more critical way for B concentrations values over 10^{18} cm^{-3} where a marked clustering process takes place.

For boron concentration $C_B \sim 10^{14} - 10^{19}$ cm^{-3}, the DXS results have shown the presence of point defects and clusters of point defects. The displacement field in the core of the cluster depends on boron concentration being stronger for lightly doped silicon; the long-range displacement field also depends on doping level, being much larger than in an r^{-2} extrapolation for heavily doped silicon. The set of the most prominent values for the cluster size varies in a range of some tens to several thousands of angstrons with an average size in general of several hundred of angstrons. The presence of the smaller clusters increases with the increasing of boron concentration.

The prevailing cluster nature depends on the parameter size and of the boron concentration. Our results are,

in general in accordance to those reported by de Kock and co-workers [7,8] for doped Czochralski silicon pulled at rates $V_g \leq 1$ mm/min. For $C_B < 10^{17}$ cm^{-3} they have verified the presence of the three types of microdefects: A (the larger), of interstitial nature, B, exhibiting a vacancy-type strain field and C (the smaller) of unravelled nature. From our results, a prevailing interstitial-nature is associated with to the observed larger clusters while the opposite occurs to the observed smaller clusters, which present a vacancy-nature. For $C_B > 10^{17}$ cm^{-3} de Kock and co-workers have observed only the presence of dislocation loops (or clusters of dislocation loops) of interstitial-nature; for $C_B \sim 10^{19}$ cm^{-3} our results also show a prevailing interstitial-type but for both larger and smaller clusters. For $C_B \sim 10^{18}$ cm^{-3} our results still show a vacancy-type for the smaller clusters; it is possible that this C_B values is related to a transition in the prevailing nature of clusters.

ACKNOWLEDGMENTS

The authors acknowledge the financial support of this work by FINEP and CNPq. They are grateful to Prof. A.M. Andrade and the staff of the Microelectronic Laboratory of Politechnic School, S. Paulo University, for supplying the silicon crystals used in the present investigation. The authors are indebted to C.A.M. Carvalho for its active support in computer programs and data processing. They want also to thank Dr. L.Q. Amaral for carefully reading the manuscript. One of the authors (BCBF) wish to thank Prof. P.A. Frugoli for helpful discussions about DXS.

REFERENCES

[1] B.O. Kolbesen, Proceedings of I Simpósio Brasileiro de Microeletrônica (1981) p. 537.

[2] A.J.R. de Kock, P.J. Roksnoer and P.G.T. Boonen, J. Crystal Growth 28 (1975) 125.

[3] S.M. Hu, J. Vac. Sci. Technol. 14 (1977) 17.

[4] J. Chikawa and S. Shirai, Japan J. Appl. Phys. 5 (1979) 153.

[5] H. Föll, U. Gösele and B.O. Kolbesen, J. Crystal Growth 52 (1981) 907.

[6] A.J.R. de Kock, P.J. Roksnoer and P.G.T. Boonen, J. Crystal Growth 22 (1974) 311.

[7] A.J.R. de Kock, W.T. Stacy and W.M. van der Wijgert, Appl. Phys. Letters 34 (1979) 611.

[8] A.J.R. de Kock and W.M. van der Wijgert, J. Crystal Growth 49 (1980) 718.

[9] D.A.W. Soares, Master Thesis, University of São Paulo, São Paulo (1980).

[10] D.A.W. Soares and C.A. Pimentel - To be published.

[11] P.H. Dederichs, J. Phys. F 3 (1973) 471.

[12] P. Ehrhart, J. Nuclear Materials 69 & 70 (1978) 200.

[13] J.R. Patel, J. Appl. Cryst. 8 (1975) 186.

[14] K. Lal and B.P. Singh, Solid State Commun. 22 (1977) 71.

[15] K. Lal and B.P. Singh, Indian J. Phys. 53A (1979) 72.

[16] K. Lal, B.P. Singh and G.H. Schwuttke, Acta Cryst. A34 (1978) S273.

[17] K. Lal, B.P. Singh and A.R. Verma, Acta Cryst. A35 (1979) 286.

[18] K. Lal and B.P. Singh, Acta Cryst. A36 (1980) 178.

[19] K. Lal and B.P. Singh, J. Crystal Growth 54 (1981) 493.

[20] B.C. Brito Filho - Master Thesis, University of São Paulo, São Paulo (1981).

[21] P.A. Frugoli - Master Thesis University of São Paulo, São Paulo (1981).

[22] C.A. Pimentel and S. Caticha-Ellis, J. Appl. Cryst. 10 (1977) 390.

[23] C.A. Pimentel and L.Q. Amaral, Nucl. Instr. & Meth. 148 (1978) 199.

[24] B.C. Larson and F.W. Young Jr., Z. Naturforsch. 28a (1973) 626.

[25] C.A. Pimentel - To be published in the Proceedings of II Simpósio Brasileiro de Microeletrônica (1982).

[26] V. Stojanoff - Private communication.

[27] P. Ehrhart and B. Schönfeld, Phys. Rev. B 19 (1979) 3896.

TABLE 1

Growth direction, resistivity and B concentration of the dislocation free doped silicon samples.

SAMPLE	GROWTH DIRECTION <hkℓ>	RESISTIVITY (Ω.cm)	B CONCENTRATION (cm^{-3})
Si 10^{14}	100	19	7.0×10^{14}
Si 10^{15}	100	9	1.5×10^{15}
Si 10^{16}	100	1	1.6×10^{16}
Si 10^{18}	111	0,015	7.0×10^{18}
Si 10^{19}	111	0,0058	2.0×10^{19}

TABLE 2

Characteristics of clusters in B doped Czochralski-Si single crystals: mean cluster size obtained from different procedures (R_{cr}, R_o, R); interstitial (I) or vacancy (V) nature related to Huang (H) or Stokes-Wilson (SW) regions (no assymetry N.A.). Slope value m from log I vs. log q plots ($\theta > \theta_B$: * ; $\theta < \theta_B$: +).

Sample	Slope (-m)				Mean Cluster Size (Å)				R (Prominent Values) × 10^2		Nature of the cluster			
	(111)		(333)		$R_{cr} \times 10$		$R_o \times 10^2$		(111)	(333)	(111)		(333)	
	H	SW	H	SW			(111)	(333)			H	SW	H	SW
Si 10^{14}	2.0	~ 2	~ 2	4.0* / 3.8+	33 ± 5* / 20 ± 3+		(11±1)×10 / 6.9±0.7	9.2 ± 5	23;12;7.0	5.9;2.7;1.9	(~N.A.)	(N.A.)	I	V
Si 10^{15}	2.1	~ 2	~ 2	3.4* / 4.0+	36 ± 5* / 25 ± 4+		33 ± 3	11.3 ± 6	32;26;15;9.1;6.2	5.3;5.1;4.0; 2.6;1.2;0.66	(N.A.)	(N.A.)	-I	V
Si 10^{16}	2.0	~ 2	~ 2* / 1.7+	~ 4	20 ± 3* / 24 ± 4+		35 ± 4	9.5 ± 5	36;25;8.7;5.2	5.8;4.8;2.6; 2.1;1.0	(~N.A.)	(N.A.)	I	V
Si 10^{18}	1.5* / 1.2+	1.5* / 1.6+	2.0* / 1.5+	2.9* / 2.4+	-		7.8±0.8	5.7 ± 3	21;20;16;14;10; 8.8;5.3;4.1;1.9	5.9;5.3;3.3; 2.9;1.1;0.79	I	V	I	V
Si 10^{19}	1.4* / 1.6+	1.7* / 1.8+	2.0* / 1.8+	2.5* / 2.5+	-		7.8±0.8	5.2 ± 3	11;9.9;7.5;6.6; 4.8;2.9;1.1	3.5;2.6;1.8; 1.3;0.97	V	I	I	I

FIGURE CAPTIONS

Fig. 1 - Double crystal X-ray diffractometer with (111) Ge monochromator and Cukα_1 beam. a) A schematic line diagram; b) (111) BLP from Ge single crystal.

Fig. 2 - Variation of width at half height ($\beta_{1/2}$) of (hkℓ) BLP from dislocation-free doped Czochralski-silicon crystal with the increase of B concentration ($\beta_{1/2}$ values from floating-zone undoped Si are indicated: —).

Fig. 3 - Typical setting of curves for DXS studies. The measurements refer to (333) relp of Si 10^{14}. a) log I vs. log q ; b) I vs. ℓn q_o where (a) corresponds to mean values; c) I vs. $1/q^2$; d) log I vs. $\Delta\theta$.

Fig. 4 - Line profile of Bragg reflections from B doped Czochralski-silicon single crystal for different B concentrations: a) (111) and b) (333) reflections.

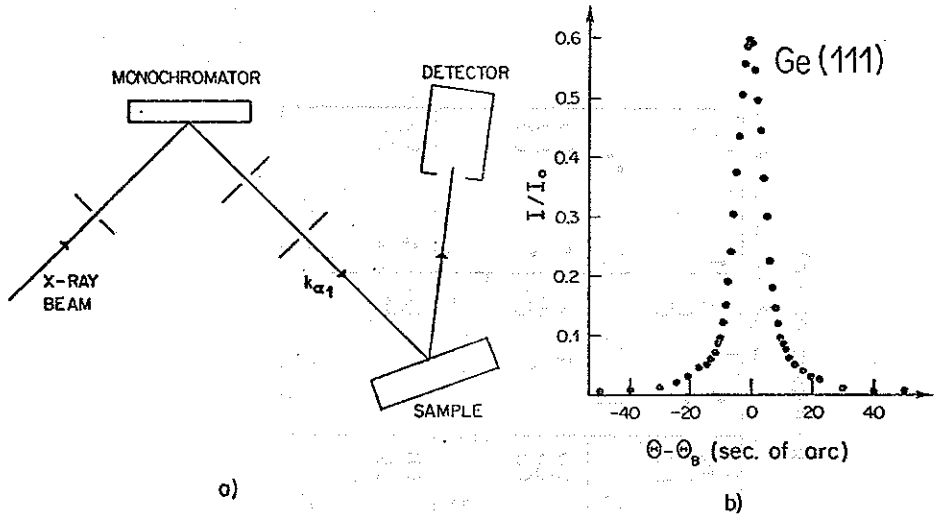

Fig. 1 - Double crystal X-ray diffractometer with (111) Ge monochromator and Cukα_1 beam. a) A schematic line diagram; b) (111) BLP from Ge single crystal.

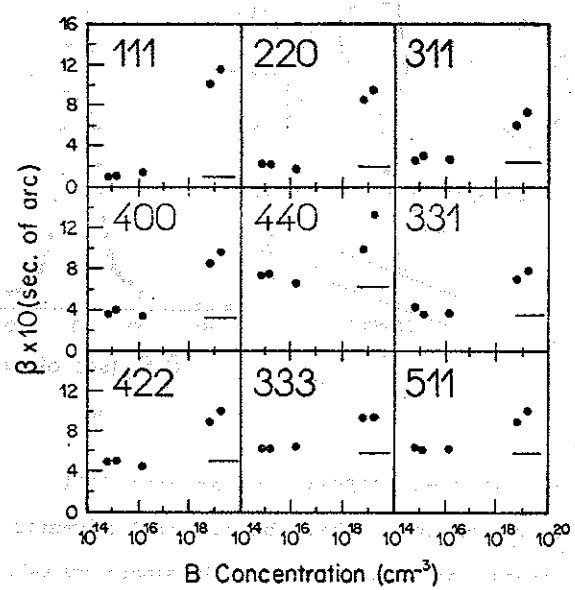

Fig. 2 - Variation of width at half height ($\beta_{1/2}$) of (hkℓ) BLP from dislocation-free doped Czochralski-silicon crystal with the increase of B concentration ($\beta_{1/2}$ values from floating-zone undoped Si are indicated: —).

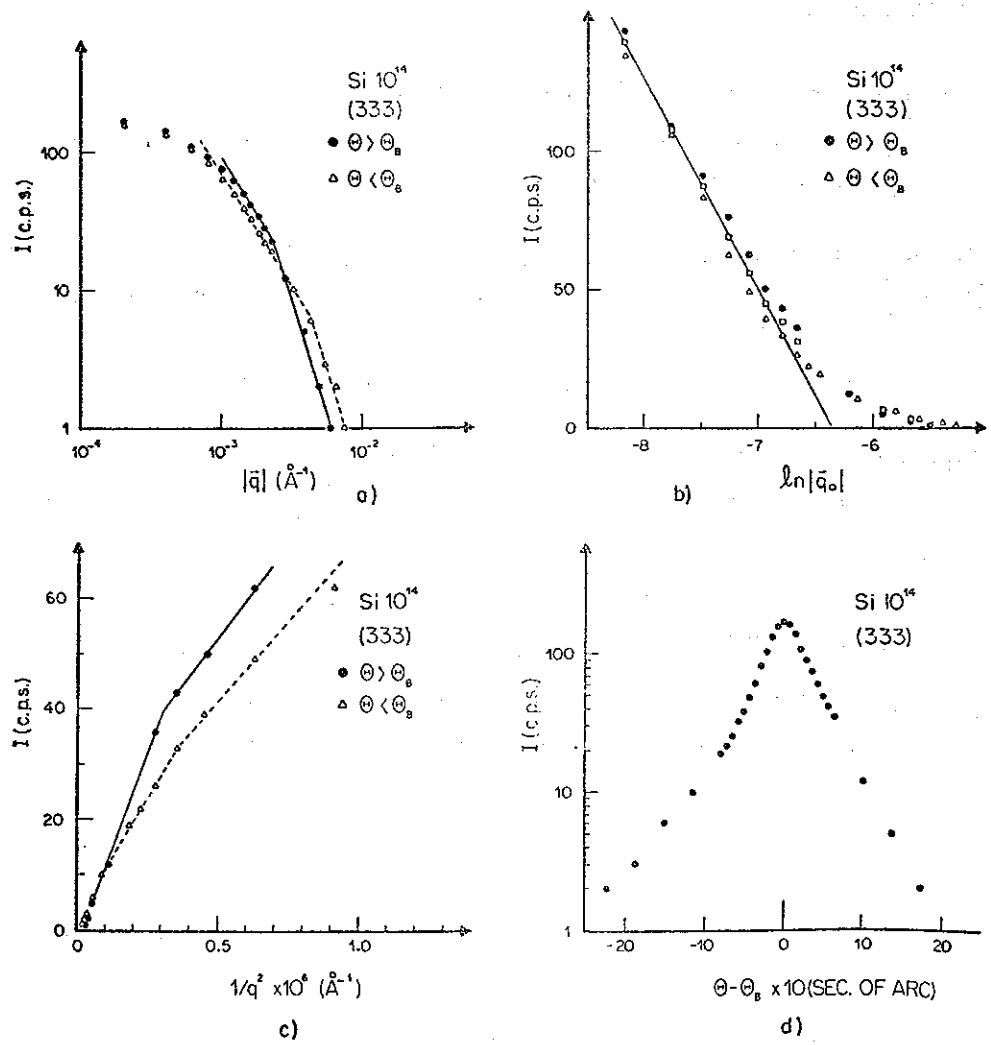

Fig. 3 - Typical setting of curves for DXS studies. The measurements refer to (333) relp of Si 10^{14}.
a) log I vs. log q ; b) I vs. ℓn q_o where (o) corresponds to mean values; c) I vs. $1/q^2$;
d) log I vs. Δθ.

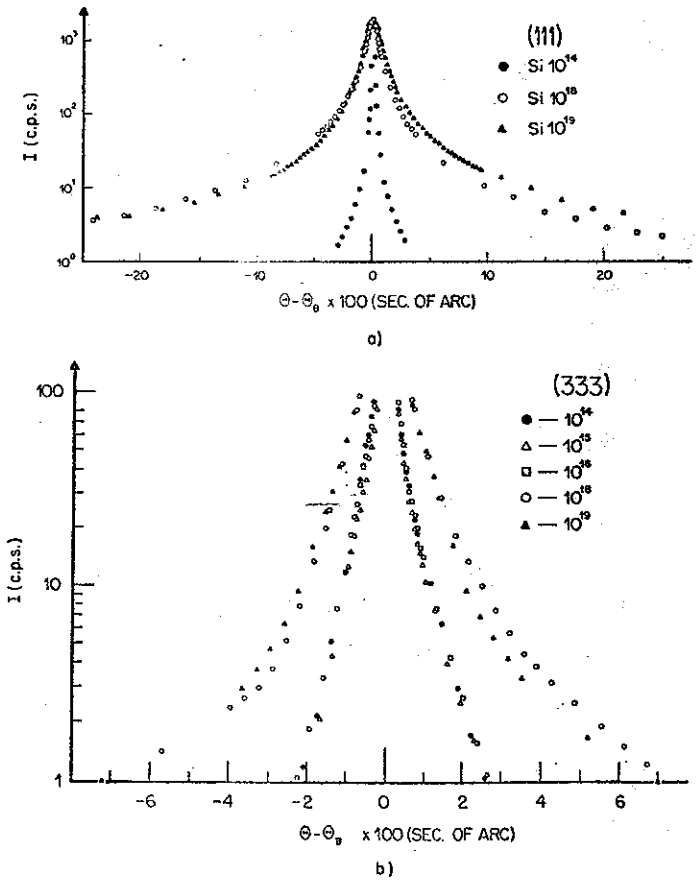

Fig. 4 - Line profile of Bragg reflections from B doped Czochralski-silicon single crystal for different B concentrations: a) (111) and b) (333) reflections.